AFRL-RD-PS-
TR-2010-1029

AFRL-RD-PS-
TR-2010-1029

Spectral Combining of Five 150W Fiber Lasers by Volume Bragg Gratings in PTR Glass

Leonid Glebov

University of Central Florida
Office of Research & Commercialization
12201 Research Parkway, Suite 501
Orlando, FL 32826-3246

01 May 2010

Final Report

APPROVED FOR PUBLIC RELEASE; DISTRIBUTION IS UNLIMITED.

AIR FORCE RESEARCH LABORATORY
Directed Energy Directorate
3550 Aberdeen Ave SE
AIR FORCE MATERIEL COMMAND
KIRTLAND AIR FORCE BASE, NM 87117-5776

NOTICE AND SIGNATURE PAGE

AFRL-RD-PS-TR-2010-1029 HAS BEEN REVIEWED AND IS APPROVED FOR PUBLICATION IN ACCORDANCE WITH ASSIGNED DISTRIBUTION STATEMENT.

LEANNE J. HENRY, Lt Col, USAF
Project Officer, Advanced Electric Lasers Branch

JORGE E. BERAUN, DR-IV
Chief, Laser Division

REPORT DOCUMENTATION PAGE			Form Approved OMB No. 0704-0188

The public reporting burden for this collection of information is estimated to average 1 hour per response, including the time for reviewing instructions, searching existing data sources, gathering and maintaining the data needed, and completing and reviewing the collection of information. Send comments regarding this burden estimate or any other aspect of this collection of information, including suggestions for reducing the burden, to Department of Defense, Washington Headquarters Services, Directorate for Information Operations and Reports (0704-0188), 1215 Jefferson Davis Highway, Suite 1204, Arlington, VA 22202-4302. Respondents should be aware that notwithstanding any other provision of law, no person shall be subject to any penalty for failing to comply with a collection of information if it does not display a currently valid OMB control number.
PLEASE DO NOT RETURN YOUR FORM TO THE ABOVE ADDRESS.

1. REPORT DATE *(DD-MM-YYYY)*	**2. REPORT TYPE**	**3. DATES COVERED** *(From - To)*
01-05-2010	Final Report	1/30/09-2/1/10

4. TITLE AND SUBTITLE	
Spectral Combining of Five 150W Fiber Lasers by Volume Bragg Gratings in PTR Glass	**5a. CONTRACT NUMBER** FA9451-09-C-0344
	5b. GRANT NUMBER N/A
	5c. PROGRAM ELEMENT NUMBER 603605
6. AUTHOR(S) Leonid Glebov	**5d. PROJECT NUMBER** 4866
	5e. TASK NUMBER LR
	5f. WORK UNIT NUMBER 13
7. PERFORMING ORGANIZATION NAME(S) AND ADDRESS(ES) University of Central Florida Office of Research and Commercialization 12201 Research Parkway, Suite 501 Orlando, FL 32826-3246	**8. PERFORMING ORGANIZATION REPORT NUMBER**
9. SPONSORING/MONITORING AGENCY NAME(S) AND ADDRESS(ES) Air Force Research Laboratory/RDLA 3550 Aberdeen Ave SE Kirtland AFB, NM 87117-5773	**10. SPONSOR/MONITOR'S ACRONYM(S)** AFRL/RDLA
	11. SPONSOR/MONITOR'S REPORT NUMBER(S) AFRL-RD-PS-TR-2010-1029

12. DISTRIBUTION/AVAILABILITY STATEMENT

APPROVED FOR PUBLIC RELEASE; DISTRIBUTION IS UNLIMITED.

13. SUPPLEMENTARY NOTES

14. ABSTRACT

The use of volume Bragg gratings (VBGs) for spectral beam combining, requires high diffraction efficiency for the diffracted beam and low diffraction efficiency for the transmitted beams simultaneously. The unique, unmatched properties of VBGs in a photo-thermo-refractive (PTR) allow spectral beam combining (SBC) achieving this condition at wavelengths with less than 0.25 nm separation. We developed a model of reflecting VBGs for high power SBC that takes into account laser spectral bandwidth, beam divergence, PTR-glass scattering losses, and grating non-uniformity.

15. SUBJECT TERMS

Bragg gratings, Spectral Beam Combining, beams, photo-thermo-refractive, spectral bandwidth, PTR-glass, grating, beam divergence.

16. SECURITY CLASSIFICATION OF:			**17. LIMITATION OF ABSTRACT**	**18. NUMBER OF PAGES**	**19a. NAME OF RESPONSIBLE PERSON**
a. REPORT	**b. ABSTRACT**	**c. THIS PAGE**			Leanne J. Henry, Lt Col, USAF
Unclassified	Unclassified	Unclassified	SAR	22	**19b. TELEPHONE NUMBER** *(Include area code)* 505-846-9302

Standard Form 298 (Rev. 8/98)
Prescribed by ANSI Std. Z39.18

This Page Intentionally Left Blank

Table of Contents

List of Figures

1. INTRODUCTION

Fundamental limits on the power that can propagate in an optical fiber such as non-linear and thermal effects leads to beam combining as the method to reach higher powers than possible from an individual fiber emitter. Spectral beam combining (SBC) and coherent beam combining are the two major complimentary methods of beam combining in the effort to reach multi-kilowatt diffraction limited beams.

The focus of this research is on spectral beam combining by volume Bragg gratings (VBGs) recorded in photo-thermo-refractive (PTR) glass. More precisely, a 750 W five channel SBC system with channel separation of 1 nm between adjacent wavelengths is the goal.

To effectively combine high power beams with such a narrow spectral separation, very precise control of the VBG resonant wavelength must be implemented. VBGs with narrow spectral selectivity also have narrow angular selectivity. So tuning the VBGs by angle becomes a challenge and is impractical at high output powers. By changing the temperature of the VBG, the glass expands or contracts, changing the period of the VBG and hence the resonant Bragg wavelength. This thermal method of tuning the resonant wavelength has much greater resolution than angle tuning and, once implemented, can be controlled electronically. Therefore, once the beams are aligned to be collinear, no realignment is necessary to tune for peak efficiency. A thermal tuning method and novel thermal tuning apparatus is presented in order to achieve precise control of the VBG resonant wavelength and hence combining efficiency of a SBC system without mechanical tuning. With this tuning method, peak combining efficiency of a given system can be maintained from low to peak power operation without mechanical realignment.

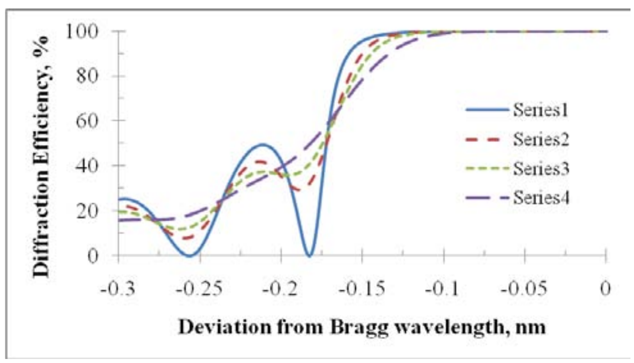

Figure 1: Modeling of VBG diffraction efficiency versus detuning from Bragg

With the necessity of increasingly narrow spectral selectivity, it is also important to model VBGs and the effects of non-ideal beams in order to optimize the design of a SBC system. When designing VBGs to be used with non-plane wave beams, there is a competition between increasing peak diffraction efficiency at the resonant wavelength for the diffracting beam and decreasing diffraction efficiency at a nearby wavelength for a transmitting beam. Series 1 in Figure 1 shows the ideal diffraction efficiency spectrum for a VBG with a very high diffraction efficiency exceeding 99.95%. Series 2 through 4 show the result of various non-ideal effects on the diffraction efficiency discussed in more detail below. The far right side of the plot shows the Bragg wavelength at which a beam would be diffracted, while the first minimum in series 1, located at -0.18 nm, shows the location of a possible wavelength at which a beam could be transmitted to combine with the diffracted beam. Without including non-ideal effects in the model, any optimization would produce unrealistic results. A VBG model that includes the three major non-ideal effects, as well as an optimization method are presented and discussed.

2. MODELING OF VOLUME BRAGG GRATINGS

There are three main effects that reduce the peak diffraction efficiency at the Bragg wavelength and raise the diffraction efficiency for the transmitted beams: laser beam divergence, spectral bandwidth, and heterogeneity of the grating parameters across the aperture of the VBG.

Figure 1 shows the influence of these three effects on the diffraction efficiency. The VBG modeled here has a thickness of 3.66 mm and a refractive index modulation of 420 ppm. Series 1 represents the monochromatic plane-wave diffraction by an ideal VBG. Series 2 is for a Gaussian beam with 2 mrad divergence. Series 3 includes 2 mrad divergence and 50 pm laser spectral bandwidth. Series 4 includes 2 mrad divergence, 50 pm bandwidth and 50 pm of resonant wavelength shift across the aperture. Understanding and minimizing these effects is important to designing an efficient system.

To include these effects in the VBG diffraction efficiency profile, the ideal plane wave diffraction efficiency spectrum is first calculated using the following equation that results from Kogelnik's theory of coupled waves [1]. For the method used here we begin with the diffraction efficiency as a function of spectral detuning from Bragg wavelength.

$$\boldsymbol{\eta}(\boldsymbol{\Delta\lambda}) = \left(\mathbf{1} + \frac{1-\left(\frac{\lambda_0 f^2 \Delta\lambda}{2 n_{av} \delta n}\right)}{sinh^2\left(\left(\frac{2\pi n_{av} t \delta n}{\lambda_0 f}\right)^2 - \left(\frac{\pi f t \Delta\lambda}{\lambda_0}\right)^2\right)^{\frac{1}{2}}} \right)^{-1} , \qquad (1)$$

where λ_0 is the resonant wavelength at normal incidence of the VBG, $\Delta\lambda$ is a small variation from the resonant wavelength, f is the grating spatial frequency, n_{av} is the average refractive index, and δn is the refractive index modulation. Angular detuning is considered to be zero here, and is introduced later through convolution. The grating spatial frequency, f, and the incident beam angle can be related by the Bragg condition given here.

$$\frac{\lambda_0}{n_{av}|\cos(\theta_m{}^*)|} = \frac{2}{f} \qquad (2)$$

where $\theta_m{}^*$ is the incident Bragg angle inside the medium [2]. Combining equations *(1)* and *(2)*, it is clear that the diffraction efficiency, η, of a given VBG can is a function of wavelength, $\Delta\lambda$, and incident Bragg angle, $\theta_m{}^*$. The notation for the diffraction efficiency then becomes $\eta(\Delta\lambda,\ \theta_m{}^*)$.

$$\boldsymbol{\eta}(\boldsymbol{\Delta\lambda}, \boldsymbol{\theta_m^*}) = \left[\mathbf{1} + \frac{1-\frac{2\Delta\lambda n_{av}\left|cos^2(\theta_m^*)\right|}{\lambda_0 \delta n}}{\sinh^2\sqrt{\left(\frac{\pi t \delta n}{\lambda_0 \left|\cos(\theta_m^*)\right|}\right)^2 - \left(\frac{2\pi t \Delta\lambda n_{av}\left|\cos(\theta_m^*)\right|}{\lambda_0{}^2}\right)^2}} \right]^{-1} \qquad (3)$$

Finite divergence and finite spectral content must be taken into account for spectral beam combining optimization. To accomplish this, the profile of the input beam in angle space is convolved with the diffraction efficiency. Let

$$\boldsymbol{G_\lambda(\Delta\lambda, w) = e^{-2\left(\frac{\Delta\lambda-\lambda_0}{w}\right)^2}} \qquad (4)$$

represent the input beam in spectral space with a Gaussian spectral profile, and

$$\boldsymbol{G_\theta(\theta, b) = e^{-2\left(\frac{\theta-\theta_0}{b}\right)^2}} \qquad (5)$$

represent the input beam in angular space with a Gaussian divergence profile, where $\boldsymbol{w}$ is the spectral width, $\boldsymbol{\theta}_0$ is incident beam angle, and $\boldsymbol{b}$ is the divergence (FWe^{-2}M – full width at the level of e^{-2} of maximum).

To include the effects of a finite beam divergence, numerical convolution is performed between equation (3) and equation (5). This process can be done analytically but we have chosen to do it numerically for computational expediency. However, before the convolution can be performed, equation (3) must be used to generate the diffraction efficiency as a function of angle detuning, Δθ. From equation (3), the diffraction efficiency as a function of wavelength detuning, Δλ, is calculated for each angle within a range of interest, producing a two dimensional diffraction efficiency array. Equation (6) and Figure 2 show the resulting array element. Notice the notation in equation six.

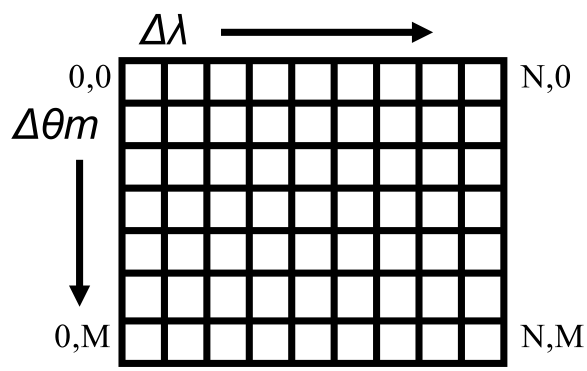

Figure 2: Diffraction efficiency array for modeling propagation of beams with finite spectral width and divergence

$$\eta(\Delta\lambda, \Delta\theta) = \left[\eta\left(\Delta\lambda, \theta^*_{m_0}\right), \eta\left(\Delta\lambda, \theta^*_{m_1}\right), \ldots\ , \eta\left(\Delta\lambda, \theta^*_{m_M}\right)\right] \qquad (6)$$

In this array, one index represents wavelength change while the other represents angle change. The variables in the array are now simply an index in the array to find the diffraction efficiency for a specified wavelength detuning and a specific angle detuning. To include the effects of a divergent beam, the Gaussian beam angular distribution in *(5)* is multiplied to each column of the array, then the area under each row is divided by the area under the Gaussian divergence curve generated by *(5)*. The resulting one dimensional array is the diffraction efficiency in wavelength space including the effects of a finite beam divergence $\boldsymbol{\eta_{d\theta}}(\Delta\lambda)$. This operation effectively convolves *(5)* and *(3)* in angular space. The process is illustrated in Figure 3, and equation (7) describes the operation.

$$\eta_{\Delta\theta}(\Delta\lambda) = \left(\eta\left(\lambda_j, \theta_i\right) * G_\theta(\theta_i, b)\ \right)(\theta_i) = \frac{\int \eta(\lambda_j, \theta_i) G_\theta(\theta_i, b) d\theta_i}{\int G_\theta(\theta_i, b) d\theta_i} \qquad (7)$$

The effects of a beam with a finite spectral bandwidth may be included by convolving the result with $G_\lambda(\lambda, w)$. The following convolution procedures are similar to the previously described procedure, with the exception that the Gaussian function is generated for many different central wavelengths and multiplied to a single diffraction efficiency profile, resulting in a modified diffraction efficiency profile, still in wavelength space.

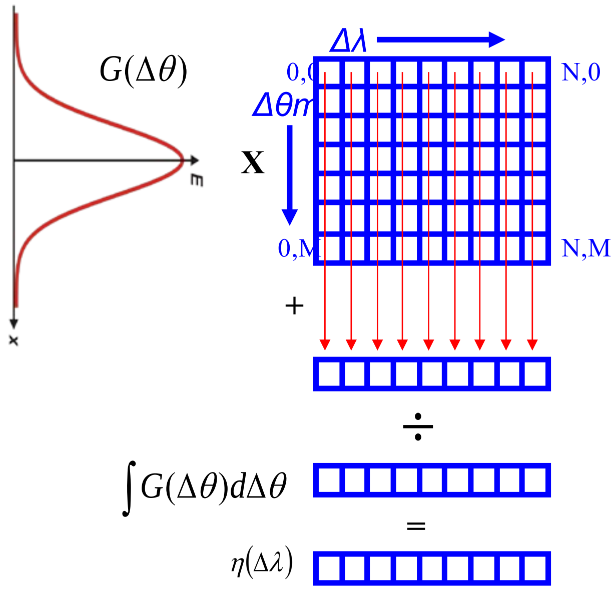

Figure 3: Numerical convolution procedure

$$\boldsymbol{\eta}_{d\lambda,d\theta}(\boldsymbol{\Delta\lambda}) = (\boldsymbol{G}_\lambda * \boldsymbol{\eta}_{d\theta})(\Delta\lambda) \qquad (8)$$

Finally, the variations in VBG Bragg wavelength across the beam aperture can be included in the model by the same mathematical method. If the shift in Bragg wavelength as a function of a lateral coordinate is assumed to be nearly linear, and the beam is Gaussian, equation *(5)* can be used again to account for this shift, where w is now the spectral shift in Bragg wavelength across the beam aperture.

A third convolution is necessary to incorporate all three effects into the model simultaneously. Equation *(6)* results from performing a second wavelength convolution on equation *(5)*.

$$\boldsymbol{\eta}_{d\lambda_B,d\lambda d\theta}(\boldsymbol{\Delta\lambda}) = \left(\boldsymbol{G}_\lambda * \boldsymbol{\eta}_{d\lambda,d\theta}\right)(\boldsymbol{\Delta\lambda}) \qquad (9)$$

Equation *(9)* gives the VBG diffraction efficiency as a function of wavelength detuning and Bragg angle, including the effects from beam divergence, beam spectral bandwidth, and a Bragg wavelength shift across the beam aperture.

3. OPTIMIZATION OF VBG FOR SPECTRAL BEAM COMBINING

A method for optimizing a spectral beam combining system with an arbitrary number of channels has been developed. In the previous section, modeling the diffraction efficiency spectrum for a single grating was discussed. The results of this modeling are used to optimize a single VBG for SBC. For a given number of laser beams, a grating configuration is found to achieve maximum efficiency by taking in account finite divergence and bandwidth of each beam along with a given spectral separation, starting wavelength, and a possible range of grating thickness and refractive index modulation. The finite divergence and bandwidth of the beams are major parameters that drive the optimization, and must be accounted for. Otherwise, ideal models could be used and no optimization would be necessary.

In a SBC system, there are as many VBGs as beams minus one. In this case, optimization must be performed for each VBG. The first VBG in the SBC system will only interact with two beams, the diffracted beam at the VBG resonant wavelength, and the transmitted beam at some specified distance from the resonant wavelength. The next VBG in the system will interact with three beams, the diffracted beam at the VBG resonant wavelength, and the two beams from the first VBG which will both transmit through the second VBG. This continues until the desired number of beams is combined. Optimization is performed iteratively for each successive VBG in the system. The output after each iteration, which is the ratio of the power incident on the optimized VBG to the power that will arrive at the next VBG for each beam, is used as the input for the next iteration. The final result of the optimization is the necessary refractive index modulation and thickness for each VBG in the system to obtain peak combining efficiency.

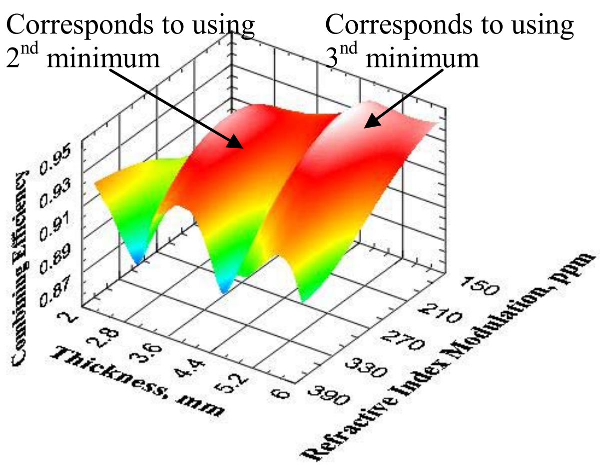

Figure 4: Efficiency of 5-channel SBC as a function of VBG thickness and refractive index modulation

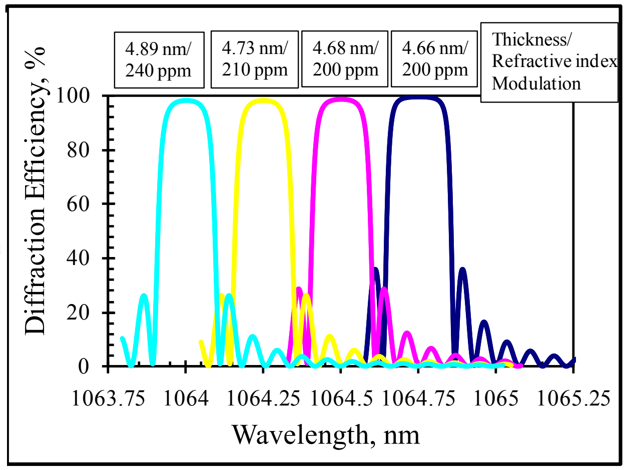

Figure 5: Diffraction efficiency spectra of VBGs for an optimized system

Figure 4 shows an example of the resulting data from an optimization calculation for a 5-channel combining system with a spectral separation between channels of 0.25 nm around 1064 nm, and beam divergence of 1 mrad. The two peaks in combining efficiency are associated with using the 2nd or 3rd minimum of diffraction efficiency curve for a transmitted beam. The results show a significant performance advantage in using the 3rd minimum, but the advantage diminishes with each successive minimum. By including scattering losses associated with grating parameters: thickness and refractive index modulation, we are able to identify an absolute maximum configuration, usually using a high order zero.

As an example, Figure 5 shows the diffraction efficiency spectrum for a system of four VBGs with channel separation of 250 pm whose parameters were determined by the optimization procedure. This system was designed such that each laser would interact with every VBG whose Bragg wavelength is less than or equal to that of the laser. Every VBG in Figure 3 has less than 1% diffraction efficiency at wavelengths corresponding to the Bragg condition of higher-wavelength VBGs.

4. THERMAL TUNING OF VOLUME BRAGG GRATINGS

We have developed a thermal tuning technique for maintaining high efficiency of beam combining throughout the power range of the system. VBGs are recorded in PTR glass which has a small but finite absorption. This means that the glass is heated under high power laser radiation, which causes glass expansion and hence Bragg wavelength shift. Therefore, when the system is aligned to operate with high efficiency at low power it must be re-aligned for high power beams to produce high combining efficiency. Using the new thermal-tuning technique, initial alignment is performed while heating the VBGs with a novel heating apparatus. As laser power is increased, the VBG temperature is lowered, and combining efficiency is maintained without need for mechanical adjustment.

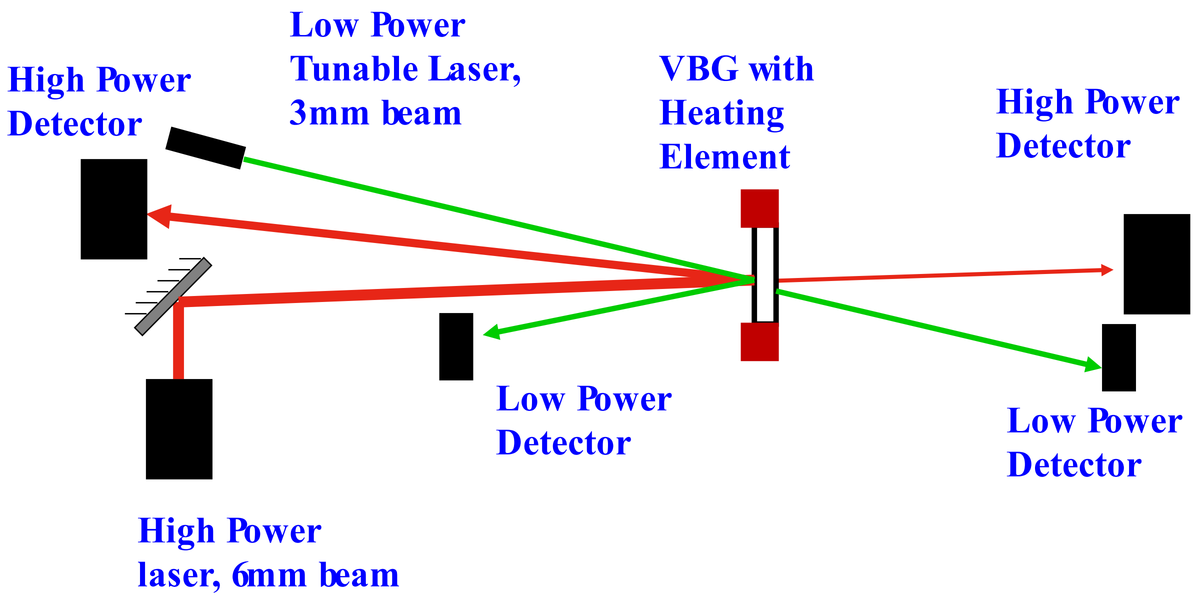

Figure 6: Experimental setup for diffraction efficiency spectra measurement in VBGs exposed to high power laser radiation

The experimental setup is shown in Figure 6. The high power laser produces a 6 mm, 160 W beam, while the low power tunable laser produces a 6 mm, ~10 mW beam with close to diffraction limit divergence. Heating of the grating may be caused by both the high power laser beam and the external heating apparatus. Diffraction efficiency spectra are measured with the tunable low power laser under various heating conditions.

Figure 7 shows the VBG diffraction efficiency spectrum for three different cases. Diffraction efficiency spectrum of grating at room temperature with no illumination by a high power radiation is shown by blue dots. Next the heater temperature is set to 70˚ C, and the VBG is aligned with a low power beam. The dashed line in Figure 5 shows the diffraction efficiency for this condition. Next the high power beam is turned on, and the heater temperature is lowered until peak diffraction efficiency is recovered to its previous position. The diffraction efficiency of a probe beam produced by a VBG under exposure to the high power beam is measured and determined to be equal to that of the low power beam. The solid line shows the diffraction efficiency spectrum of the VBG with the high power beam turned on and the heater temperature set to 55˚ C. The two curves overlap, demonstrating the conservation of resonance wavelength from low to high laser power.

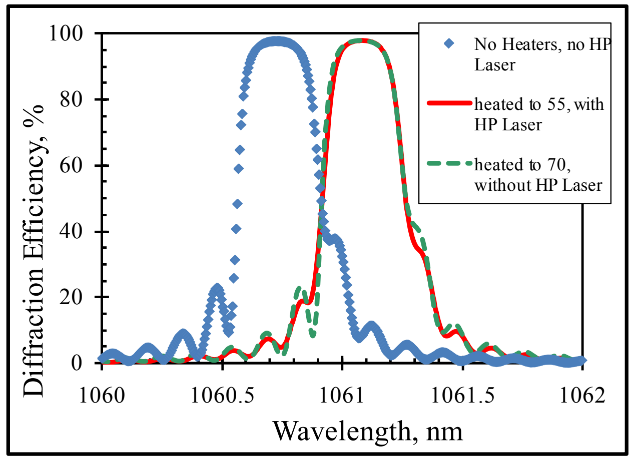

Figure 7: Diffraction efficiency under various heating conditions

Using this thermal tuning apparatus, the laser heats the glass from the center while the glass temperature is controlled from the edge. Without the use of thermal control, the temperature at the edge of a VBG under high power laser radiation is much cooler than the temperature at the peak of radiation. This thermal gradient produces a gradient in the Bragg wavelength of the VBG which can reduce combining efficiency. By heating the edge of the grating while high power radiation heats the center, the combined thermal gradient will be smaller than it would be without thermal control.

The experimental setup in Figure 6 is modified by replacing the low power output collimator which produces a 6 mm beam with one which produces a 3 mm beam. With a smaller test beam, different parts of the VBG can be probed more accurately.

Figure 8 shows the Bragg wavelength shift as a result of heating across the grating aperture while the VBG is under various heating conditions. The Bragg wavelength shift is the difference between the Bragg wavelength of the VBG at room temperature and under a given external heating.

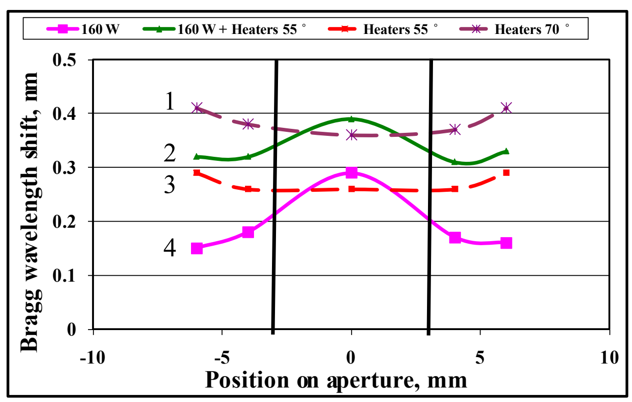

Figure 8: Bragg wavelength profile across the aperture:

1. 0W laser power, heating to 70° C
2. 160W laser power, heating to 55° C
3. 0 W laser power, heating to 55° C
4. 160 W laser power, no heating

The lower solid pink line shows the Bragg shift as a result of heating from only the laser source. Next the grating is pre-heated to a desirable starting temperature. The upper dashed line shows the Bragg wavelength profile while being heated from the edge to 70°C. When the laser radiation is turned on, the VBG edge temperature is reduced to 55°C. The Bragg wavelength profile that results from both high power laser radiation and heating at the edge is shown by the upper solid line (green). The Bragg wavelength gradient between the center and the edge of the VBG is significantly reduced in this case. Also, the resulting central Bragg wavelength is very near the intended central Bragg wavelength, and therefore diffraction efficiency is maintained without angle tuning the grating or spectrally tuning the laser.

The temperature of 55° C was found by lowering the temperature from 70° C until peak diffraction efficiency was restored. However, this temperature returned the central Bragg wavelength to just above the original Bragg wavelength associated with heating to 70°C without the high power laser. This is a result of the Gaussian-like thermal profile the beam produces. The average deviation from this central wavelength from the edge of the beam to the center is minimized to achieve peak diffraction efficiency. Figure 9 illustrates this effect.

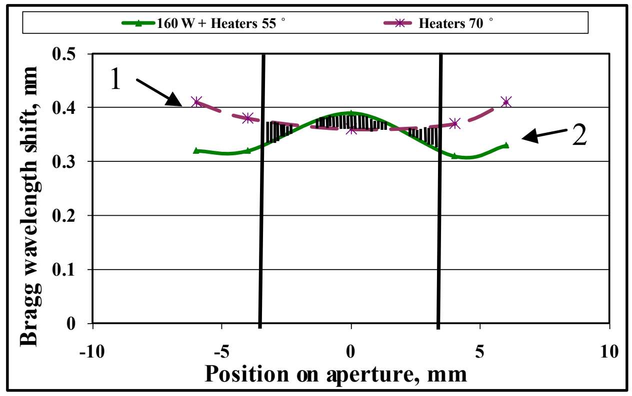

Figure 9: Profiles of deviation from initial Bragg wavelength for:
1. External heating to 70°C and
2. A combination of external heating to 55°C and 160 W laser radiation

The beam quality of the test beam was measured to determine any effect the thermal tuning apparatus may have. Table 1 below shows the peak diffraction efficiency and M^2 under various heating conditions. It is clear from these results that the thermal tuning method does not deteriorate beam quality. The first three rows are the results of changing the VBG edge temperature without any high power radiation, while the final two rows show the results with high power radiation at two different VBG edge temperatures. In all cases, $M^2 \leq 1.12$, and diffraction efficiency was near 98%. For the case of using a high power beam without any thermal control of the VBG, row four, the diffraction efficiency dropped down to 97.7%. This is the case associated with the highest thermal gradient across the aperture of the beam. The final case, row five, using high power radiation and thermal control of the VBG, reduces the thermal gradient and returns the diffraction efficiency to 98%.

Table 1: Diffraction efficiency and M^2 under various heating conditions

Incident optical power	**Edge Temperature**	**Diffraction Efficiency**	**Test Beam M2**
0 W	**~25˚ (heater off)**	**98.0%**	**1.12**
0 W	**70˚ (heater on)**	**98.0%**	**1.09**
0 W	**55˚ (heater on)**	**98.0%**	**1.10**
160 W	**~37˚ (heater off)**	**97.7%**	**1.12**
160 W	**55˚ (heater on)**	**98.0%**	**1.09**

5. **SPECTRAL BEAM COMBINING BY THERMAL TUNING OF VBGs**

The thermal tuning technique, described in detail in section 5, can be used in spectral beam combining to keep the gratings in resonance from low power up to the full power of a given SBC system. Formerly, a SBC system would be aligned such that peak combining efficiency is achieved only after the VBGs heat up under high power laser radiation and reach thermal equilibrium. In this case, any fine tuning of the system would require angular adjustments to the VBGs while maintaining full input laser power. Angle tuning a VBG by hands while kW-level

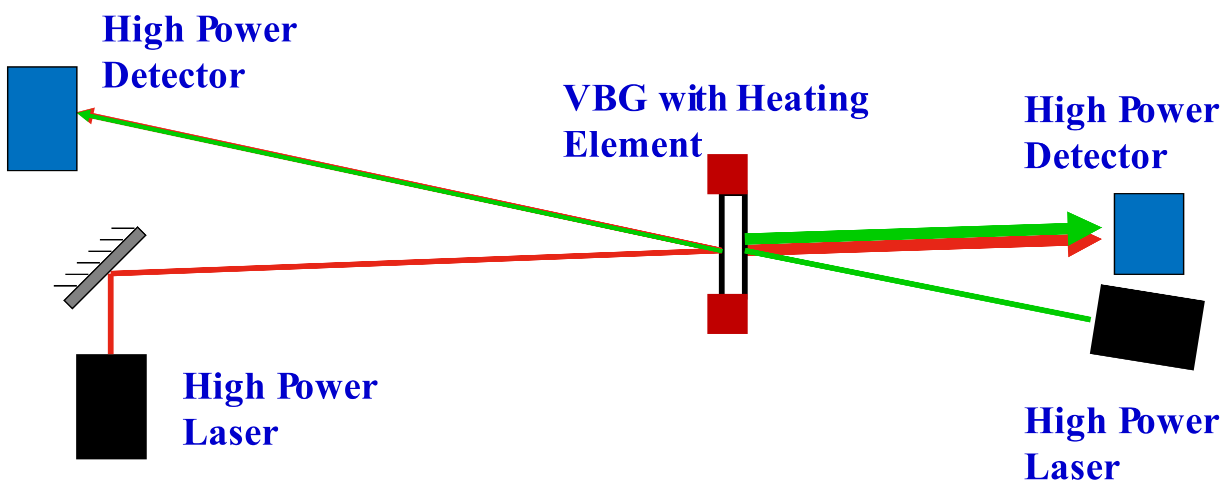

Figure 10: Two channel high power SBC experimental setup

radiation is incident on the grating is not convenient. Thermal tuning eliminates the need for mechanical tuning and may be electronically controlled with proper feedback. Mechanical alignment is used only to make each beam co-linear, while thermal tuning is used to maintain peak combining efficiency throughout the power range of the system.

Figure 10 shows the experimental setup for 2 channel high power spectral beam combining. One VBG with thermal tuning is used to combine two high power lasers. Figure 11 shows the optimal VBG edge temperature as a function of power level. The combining efficiency for each data point is also given. From 10 W to over 300 W, beam combining efficiency was maintained within 0.5% of the low power combining efficiency. No angular tuning was required to maintain combining efficiency.

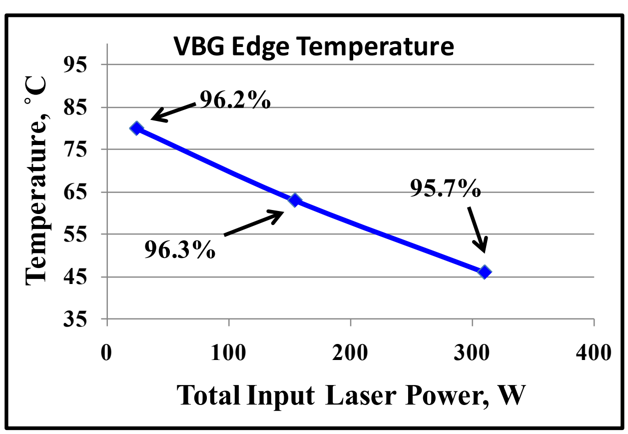

Figure 11: Two channel beam combining efficiency at different power levels and VBG edge temperatures

The thermal tuning setup was first expanded to 5 low-power channels. The total combining efficiency was greater than 90%, and the combined beam had $M^2 < 1.1$. Figure 12 shows the beam quality test results for the 5 combined low power beams.

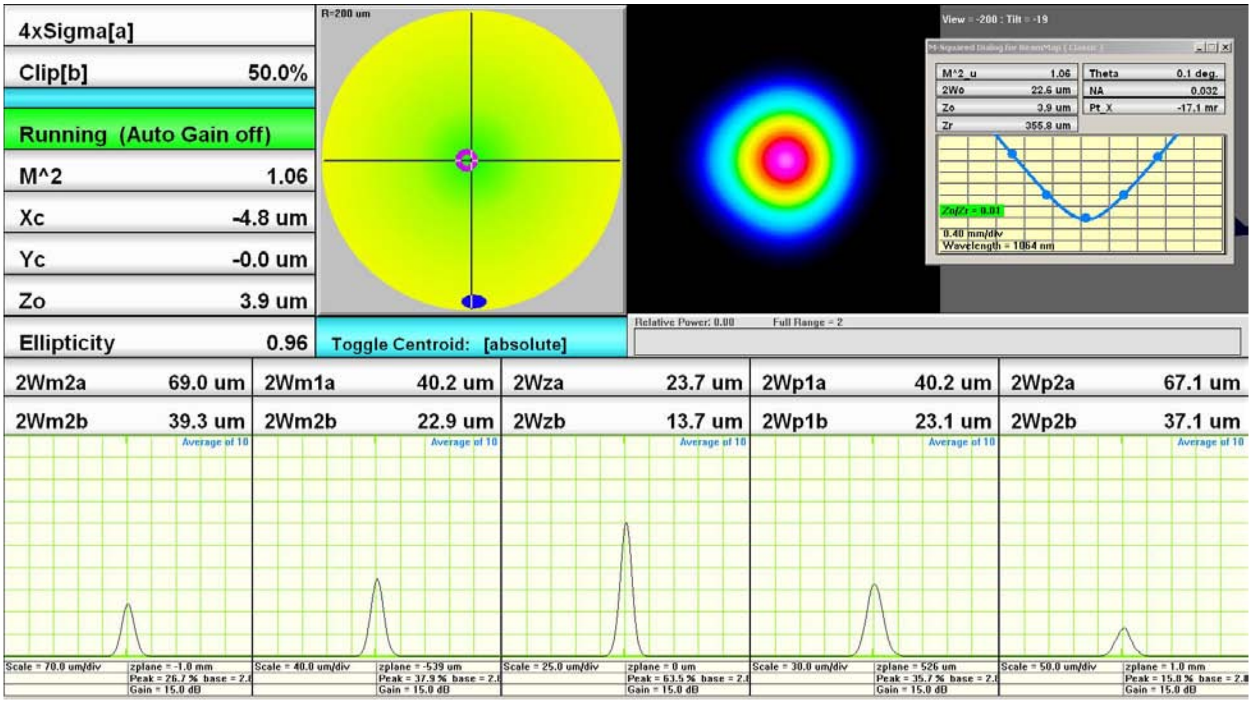

Figure 12: Five channel, combined low power beam quality, M^2=1.06

6. FIVE-CHANNEL HIGH-POWER SPECTRAL BEAM COMBINING

The next step was to apply the VBGs thermal tuning approach to 5 channel high-power beam combining set-up. Figure 13 demonstrates the arrangement of the beams and their corresponding VBGs. We used the same tuning procedure based upon minimizing the diffraction losses behind the VBGs, in order to achieve maximum efficiency.

To incorporate the spectral beam combining setup in the AFRL fiber lasers testbed, a set of seed lasers was designed and fabricated at IPS Corporation. The seed lasers chosen for use with the AFRL amplifiers are wavelength stabilized diode lasers. Each laser used a VBG, contained inside the diode packaging, as an output coupler to select the central wavelength and to narrow the diode laser bandwidth. All VBGs were fabricated by Optigrate Corporation and supplied to IPS. Each laser was coupled to a single mode polarization maintaining fiber for input to the AFRL amplifiers.

Each seed laser produced a beam with an output power of greater than 60 mW at 300 mA, a spectral bandwidth of 0.02 nm, had a slope efficiency of more than 0.2 W/A, and had a threshold current of 25 mA. Beam combining optics were designed for a spectral separation between channels of 1 nm, therefore a bandwidth of 0.02 nm was sufficiently narrow to avoid cross talk between channels. The wavelengths of the lasers were 1062.45 nm, 1063.39 nm, 1064.25 nm, 1065.40 nm, and 1066.26 nm. The small differences in channel separation were easily accommodated by a combination of precise thermal and angular tuning of the VBGs. All these

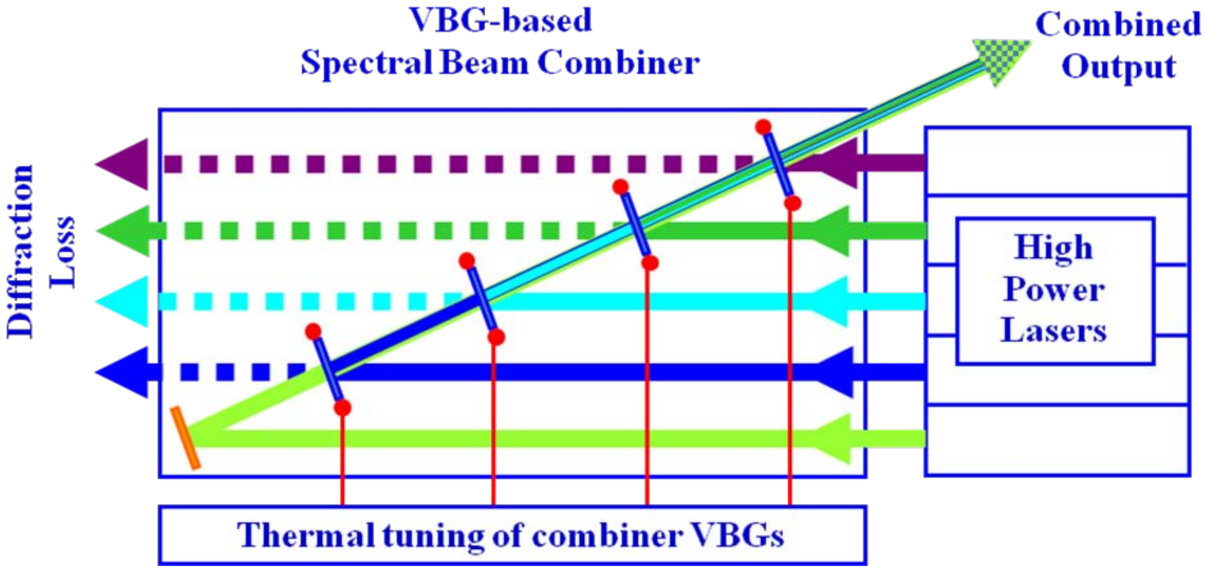

Figure 13: 5 beam high-power beam spectral beam combining scheme

lasers were coupled to the AFRL fiber testbed system with five fiber channels amplified at the mentioned fixed wavelengths.

This spectral beam combining system was mounted on a breadboard and originally assembled at CREOL/UCF. Its efficiency and beam quality for the low power laser beams was studied. It was found that the system provided combining efficiency exceeding 90% with the beam quality (M^2) of the combined beam been approximately 0.2 larger than that for the worst of the original beams. The thermal tunability of each grating was approximately ±0.3 nm. This system was sent to AFRL and incorporated in the fiber lasers testbed.

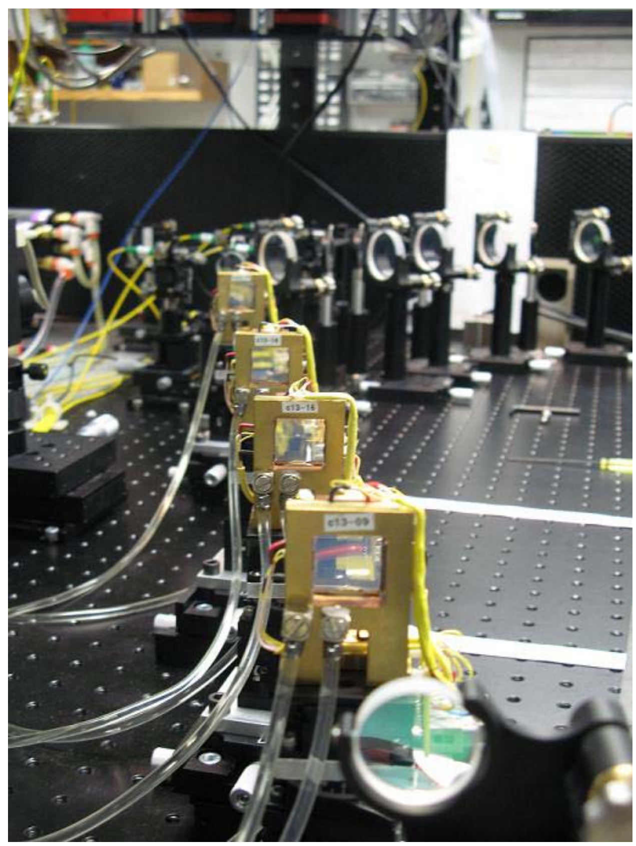

Figure 14: Photo of the combining setup depicted in Fig. 13

Figure 14 shows the set up from the perspective of the back side of the VBGs. The mirrors seen in the far end were used to divert the high-power beams towards the gratings due to specificity of the lasers/setup orientation. The water cooling lines enabling low temperatures for the back sides of the thermo-electric coolers (TECs) attached to each side of the gratings are also well seen. The temperature of each side of each grating was monitored and was used as feedback information for keeping the TECs at the same temperatures. Experiments investigating the combining efficiency and the final beam M^2 were performed at different power levels. The efficiency achieved was equal to or better than 90%, reaching 93% at a total combined power of 460 W (Fig. 15). The tuning of the set-up after the initial low-power alignment was made through adjustment of the gratings' temperatures and through monitoring of the diffraction losses behind each grating.

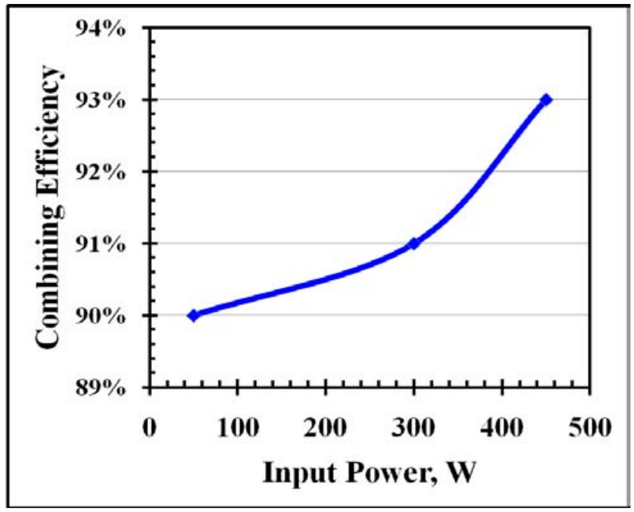

Figure 15: Total efficiency of 5 beam spectral beam combining set-up at different power levels

The second important parameter describing how good a beam combining scheme is performing is the M^2 of the output beam. Our experiments demonstrated that regardless of the power levels at which the lasers were operating the combined M^2 was always only 0.2 higher than the M^2 of the worse input beam. This proves that the distortions introduced by the VBGs are minimal even at powers reaching hundreds of watts.

7. CONCLUSION

Modeling of volume Bragg gratings, optimization of spectral beam combiner parameters, and temperature tuning of VBGs have enabled a demonstration of a robust and portable 5 channel SBC system incorporated into the fiber lasers testbed at AFRL. This system was aligned at low power and showed 96% diffraction efficiency with a diffraction limited beam quality. The same thermally tuned, beam combining set-up was used to demonstrate 93% efficiency at a maximum power of 460 W and a beam quality purely limited by the power and beam quality of the combined beams.

REFERENCES

[1] Kogelnik, and Herwig, "Coupled wave theory for thick hologram gratings," Bell System Technical Journal, 48(9), 2909-2947 (1969).

[2] Igor V. Ciapurin, Leonid B. Glebov, Vadim I. Smirnov. Modeling of phase volume diffractive gratings, part 1: transmitting sinusoidal uniform gratings. Optical Engineering 45 (2006) 015802, 1-9.

DISTRIBUTION LIST

DTIC/OCP 8725 John J. Kingman Rd, Suite 0944 Ft Belvoir, VA 22060-6218	1cy
AFRL/RVIL Kirtland AFB, NM 87117-5776	2 cys
Official Record Copy AFRL/RDLA/Leanne J. Henry	1 cy

This Page Intentionally Left Blank